Available online at www.sciencedirect.com
SCIENCE DIRECT®
Journal of volcanology and geothermal research
Journal of Volcanology and Geothermal Research 131 (2004) 241–264
www.elsevier.com/locate/jvolgeores

Anatomy of a lava dome collapse: the 20 March 2000 event at Soufrière Hills Volcano, Montserrat

S.A. Carn [a,b,*], R.B. Watts [b,c], G. Thompson [b,d], G.E. Norton [b,d]

[a] *Joint Center for Earth Systems Technology (NASA/UMBC), University of Maryland Baltimore County, 1000 Hilltop Circle, Baltimore, MD 21250, USA*
[b] *Montserrat Volcano Observatory, Fleming's, Montserrat W.I.*
[c] *Department of Geology, University of South Florida, 4202 East Fowler avenue, SCA 528, Tampa, FL 33620, USA*
[d] *British Geological Survey, Keyworth, Nottingham NG12 5GG, UK*

Received 1 October 2002; accepted 26 September 2003

Abstract

A second extrusive phase of the currently ongoing 1995–2003 eruption of Soufrière Hills Volcano (SHV), Montserrat, commenced in mid-November 1999 following ~19 months during which no fresh lava had reached the surface. By mid-March 2000, a new andesite lava dome constructed within a collapse scar girdled by remnants of the 1995–1998 dome complex had attained an estimated volume of $\sim 29 \pm 3$ million m^3 (Mm^3). On 20 March 2000, during a period of heavy rainfall on the island, a significant collapse event ensued that removed ~95% of the new lava dome ($\sim 28 \pm 3$ Mm^3) during ~5 hours of activity that generated ~40 pyroclastic flows and at least one magmatic explosion. The associated ash cloud reached an altitude of ~9 km and deposited ash on the island of Guadeloupe to the southeast, and a number of lahars and debris flows occurred in valleys on the flanks of SHV. A large quantity of observational data, including contemporaneous field observations and continuous data from the broadband seismic network on Montserrat, allow a detailed reconstruction of this dome collapse event. In contrast to most of the large dome collapses at SHV, the 20 March 2000 event is distinguished by a lack of short-term precursory elevated seismicity at shallow depths beneath the lava dome. Broadband seismic amplitude data recorded during the event are used to infer the cumulative volume of collapsed dome as the collapse progressed. These data indicate that the high-velocity pyroclastic flows observed at the climax of the event removed by far the largest portion (~68%) of the lava dome at peak discharge rates (estimated from the seismic record) of $\sim 2 \times 10^4$ m^3 s^{-1}. Following the 20 March 2000 collapse, lava dome growth recommenced immediately and continued without significant interruption until another, larger dome collapse occurred on 29 July 2001. The 29 July 2001 event also coincided with heavy rainfall on Montserrat [Matthews et al. (2002) Geophys. Res. Lett. 29; DOI:10.1029/2002GL014863] and lacked precursory elevated seismic activity. We attribute the initiation of the 20 March 2000 collapse to a prolonged spell of heavy rainfall on the lava dome prior to and during the event. The precise causal mechanism remains controversial, though some combination of mechanical erosion and/or destabilization of a critically poised face of the lava dome, the action of pressurized steam or water on potential failure surfaces within the dome, rapid cooling of hot lava and small phreatic explosions seems likely. Anecdotal evidence exists for other rainfall-induced activity on Montserrat, and the triggering of explosive or pyroclastic flow activity by rainfall has been noted at dome-forming volcanoes elsewhere, including Merapi, Indonesia [Voight et al. (2000) J. Volcanol. Geotherm. Res. 100, 69–138], Unzen, Japan [Yamasato

* Corresponding author. Fax: +1-410-455-5868. *E-mail address:* scarn@umbc.edu (S.A. Carn).

0377-0273/03/$ – see front matter
doi:10.1016/S0377-0273(03)00364-0

et al. (1997) Papers Meteorol. Geophys. 48], Santiaguito, Guatemala [Smithsonian Institution Global Volcanism Network Bull. 15 (1990)] and Mount St. Helens, USA [Mastin (1994) Geol. Soc. Am. Bull. 106, 175–185]. Hazard mitigation plans at dome-forming volcanoes would therefore benefit from the inclusion of meteorological forecasting and rain monitoring equipment, particularly in the tropics.

Keywords: Montserrat; lava dome; dome collapse; volcanic activity; rainfall; volcanic hazards

1. Introduction

Pyroclastic flows and surges resulting from lava dome collapses are the salient hazard in areas surrounding dome-forming volcanoes. Dome collapses can also trigger, or be triggered by, explosive activity, which is a common feature of dome-forming eruptions (Christiansen and Peterson, 1981; Newhall and Melson, 1983; Miller and Chouet, 1994; Sparks, 1997; Voight and Elsworth, 2000) and can result in column-collapse pyroclastic flows and drifting ash clouds that are a significant hazard to aviation (e.g. Casadevall, 1994). The sudden onset of these events and the highly destructive nature of the resulting pyroclastic flows and surges (e.g. Yamamoto et al., 1993; Cole et al., 1998; Abdurachman et al., 2000) calls for accurate methods of forecasting them, yet such methods are still in their infancy.

Development of predictive techniques requires intensive monitoring of active lava domes using a variety of geophysical datasets (e.g. Voight et al., 2000b), and observation of the current eruption of Soufrière Hills Volcano (SHV) on Montserrat, West Indies (Fig. 1) by the Montserrat Volcano Observatory (MVO) has resulted in some significant advances in our understanding of lava dome collapse triggers (e.g. Voight et al., 1998; Watts et al., 2002) at a highly instrumented and well-monitored volcano. However, surveillance of the SHV eruption and other dome-forming eruptions (e.g. Merapi, Indonesia) has also shown that not all lava dome collapse events display the same patterns and the 'predictability' of dome collapses is thus quite variable. A significant and sustained, yet unpredicted dome collapse occurred at SHV on 20 March 2000. This event differed from earlier collapses of the SHV lava dome during periods of active dome growth in that it lacked the short-term precursory activity that had characterized most of the earlier events (Table 1), though it did coincide with a period of exceptionally heavy rainfall on Montserrat.

The first historic eruption of SHV (Fig. 1) began in July 1995 and was continuing at the time of writing. This eruption has, to date, involved two prolonged phases of andesitic lava dome growth at the volcano's summit. Phase 1 had commenced unequivocally by November 1995 and continued until March 1998, involving vigorous dome growth, pyroclastic flows and surges, Vulcanian explosions and one debris avalanche that triggered a lateral blast on 26 December 1997 (Young et al., 1998; Druitt et al., 2002; Woods et al., 2002). A period of residual activity, comprising dome degradation and further explosive events but virtually no extrusion of fresh lava, followed this first phase of dome growth (Norton et al., 2002) and continued until November 1999 when fresh andesitic magma once again began to extrude amidst the remains of the previous lava dome (Fig. 2a). As of July 2003, this latest phase of dome growth is currently ongoing.

The two phases of lava dome extrusion at SHV have exhibited marked differences in eruptive style. Phase 2 has generally involved more stable

Fig. 1. Map of Montserrat showing features mentioned in the text. Deposits emplaced during the 1995–1999 period of activity are shaded (see key); activity from November 1999 until the 20 March 2000 collapse was almost entirely confined to the Tar River Valley. Inset map shows location of Montserrat in the Lesser Antilles island arc and the dashed box indicates the region covered by the GOES satellite images in Fig. 6.

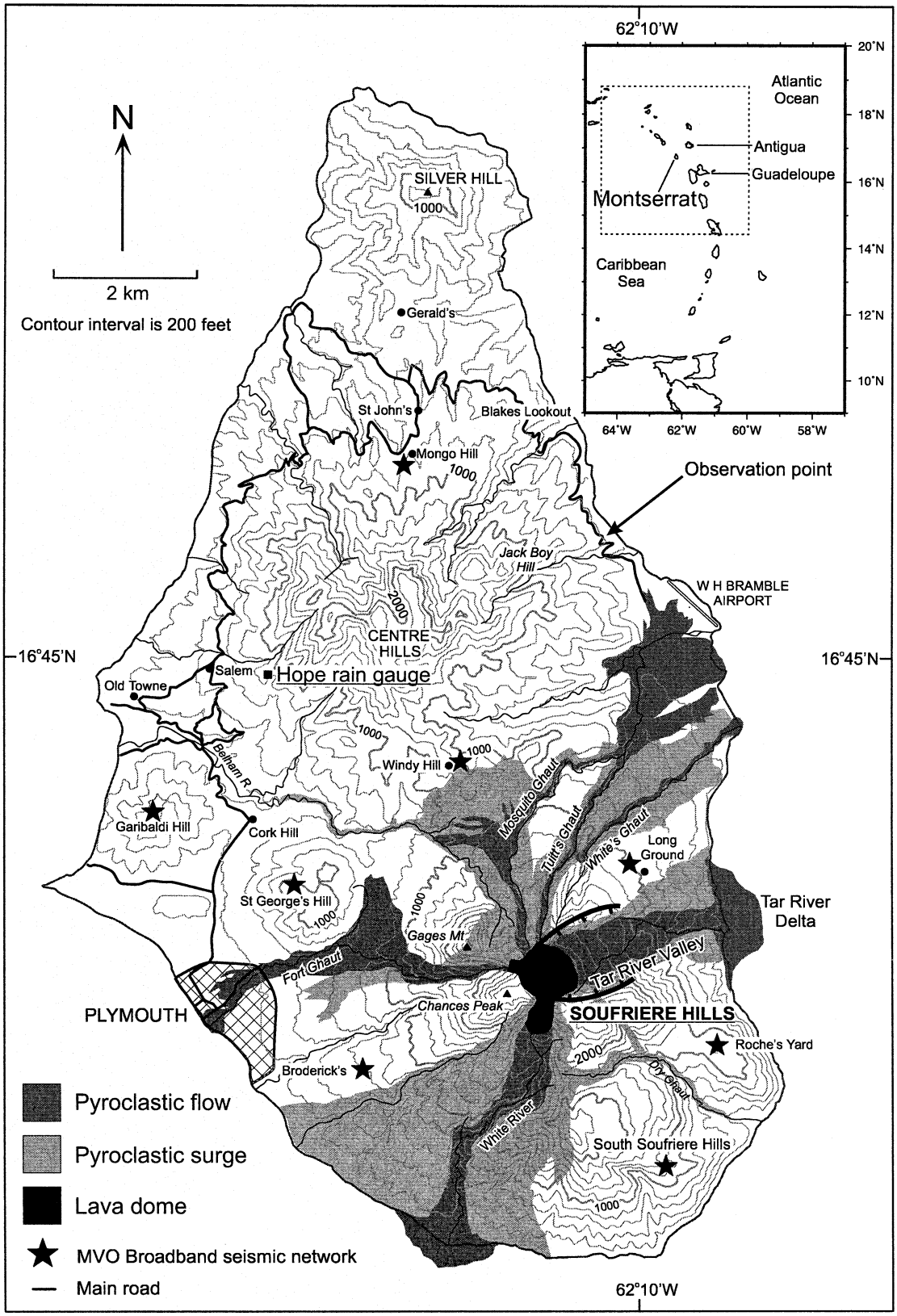
62°10'W
N
2 km
Contour interval is 200 feet
SILVER HILL
1000
Gerald's
St John's
Blakes Lookout
Mongo Hill
1000
Observation point
Jack Boy Hill
2000
CENTRE HILLS
W H BRAMBLE AIRPORT
16°45'N
Salem
Hope rain gauge
Old Towne
1000
Belham R.
Windy Hill
1000
Garibaldi Hill
Cork Hill
McSquito Ghaut
Tuitt's Ghaut
White's Ghaut
Long Ground
St George's Hill
1000
Gages Mt.
Tar River Delta
Tar River Valley
Fort Ghaut
PLYMOUTH
Chances Peak
SOUFRIERE HILLS
Roche's Yard
2000
Broderick's
Dry Ghaut
White River
South Soufriere Hills
1000
Pyroclastic flow
Pyroclastic surge
Lava dome
MVO Broadband seismic network
Main road
Atlantic Ocean
Antigua
Guadeloupe
Montserrat
Caribbean Sea
20°N
18°N
16°N
14°N
12°N
10°N
64°W
62°W
60°W
58°W

Table 1
Largest sustained dome collapses of the 1995–2003 SHV eruption (as of April 2003), in order of decreasing volume

Date	Collapse vol. (Mm^3)	Pf runout[a] (km)	Hybrid swarms[b]	Rainfall[c]	Duration (min)
26 December 1997	46	≥4.5 (SSW)	y	n	15–30
29 July 2001	45	≥3.5 (E)	n	y	300
20 March 2000	28	≥3.5 (E)	n	y	240
3 July 1998	15–19	≥3.5 (E)	n	y	150
21 September 1997	14	≥6.9 (NE)	y	n	20–30
17 September 1996	9.5	≥2.5 (E)	y	n	480–540
3 August 1997	7	≥5 (W)	y	n	120–150
8 December 2002	5	≥4 (NE)	n	n	n/a
25 June 1997	4.9	6.7 (N/NE)	y	n	25
6 November 1997	4.6	≥4.5 (SSW)	y	n	35

Compiled from Calder et al. (1999), Cole et al. (2002) and MVO (unpublished data, 2002).

[a] Pf = pyroclastic flow. A runout distance of ≥x km indicates that flows entered the sea x km from the dome. Approximate direction of flow movement is also given.

[b] Indicates whether hybrid earthquake swarms were recorded before the collapse.

[c] Indicates whether the collapse coincided with significant rainfall.

dome growth and significantly fewer periods of vigorous pyroclastic flow and collapse activity than phase 1, allowing the active dome to attain larger volumes during phase 2. Nevertheless, phase 2 has to date been interrupted by two major dome collapse events (20 March 2000 and 29 July 2001), each of which removed 30–50 million m^3 [Mm^3] of the active dome, producing high-velocity pyroclastic flows, significant ash clouds and extensive lahars and debris flows. Both of these events lacked the short-term precursory seismic signals during the build-up to the collapse that were typically observed prior to phase 1 collapse episodes (Table 1; e.g. Miller et al., 1998; Voight et al., 1998, 1999) and as such were difficult to predict. However, both the 20 March 2000 and 29 July 2001 collapses coincided with periods of exceptionally intense rainfall on the island, and we implicate this in the triggering and prolongation of these events (Matthews et al., 2002). A large collapse of the lava dome on 3 July 1998, whilst there was no active dome extrusion, is also thought to have been initiated by heavy rainfall (Table 1; Norton et al., 2002). Rainfall-induced activity has been suspected at other active dome-forming volcanoes (e.g. Merapi and Unzen; Voight et al., 2000a,b; Ratdomopurbo and Poupinet, 2000; Yamasato et al., 1997) and may be a previously underestimated hazard during and after this type of eruption.

In this paper we reconstruct the 20 March 2000 dome collapse using a combination of eye-witness observations, continuous broadband seismic data, and satellite images of the ash clouds produced. Calibration of the seismic data with the total volume removed by the collapse allows us to estimate the volume and discharge rates of individual pyroclastic flows generated during the event. We then discuss the evidence linking the 20 March 2000 collapse to rainfall, review the reported instances of rainfall-induced activity at other volcanoes, and propose a simple model for a rainfall-triggered dome collapse. Note that we use the term 'dome collapse' in this paper to describe a sustained event comprising many individual large rockfalls and pyroclastic flows and other related activity over a period up to a few hours in duration. Gravitationally unstable lava domes typically shed material (and are thus collapsing) near-continuously, though the individual rockfalls and pyroclastic flows produced are usually of low volume and low energy.

2. Data

In our analysis we use data from the digital broadband seismic network on Montserrat. MVO's digital seismic network consists of eight stations (Fig. 1). Stations MBBY (Broderick's),

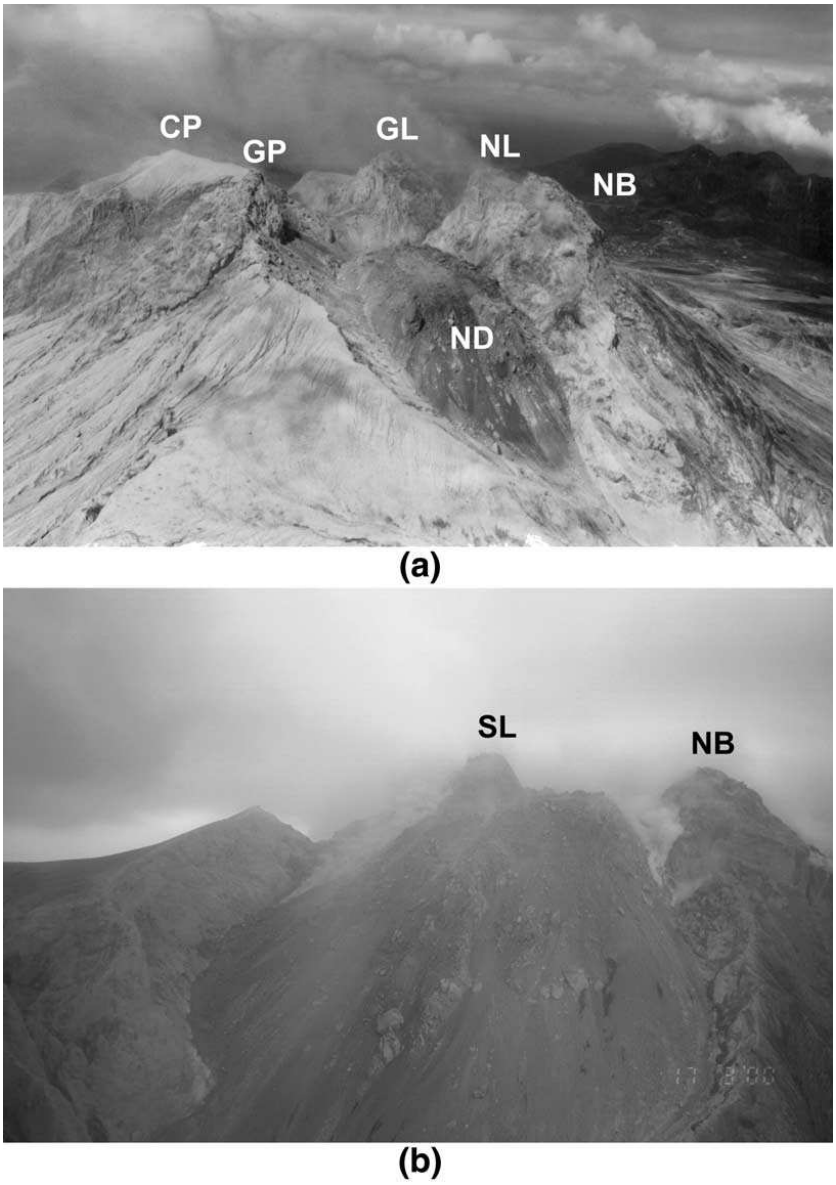

Fig. 2. (a) View of the young N99 dome (ND) on 16 December 1999. The dome grew within the large scar formed by dome collapses and explosions during the 20-month period of residual activity (Norton et al., 2002). View direction is towards the NW, and the four remaining lobes of the 1995–1998 phase of dome growth (the Northeast Buttress (NB), Northern Lobe (NL), Gages Lobe (GL) and Galway's Peak (GP)) are indicated along with Chances Peak (CP; Fig. 1). (b) View of the eastern flank of the N99 dome on 17 March 2000, looking ~SW from above the Tar River Valley. By this time the dome had increased in height substantially and dome growth was focused on the southern lobe (SL; note rockfall sourced from the lobe directed ~S towards the crater rim), whilst rockfall activity on the eastern flank had ceased. The Northeast Buttress (NB) is marked for reference to (a).

MBRY (Roche's Yard), MBGH (St George's Hill) and MBGB (Garibaldi Hill) have Guralp CMG-40T seismometers, which have three components and a corner frequency of 30 s. Stations MBLG (Long Ground), MBMH (Mongo Hill), MBSS (South Soufriere Hills) and MBWH (Windy Hill) have Integra LA-100 seismometers, which have a vertical component only and a corner frequency of 2 s. The sampling frequency is 75 Hz and an anti-aliasing filter is applied at 30 Hz.

Analog-to-digital conversion, telemetry and recording are all 24-bit, giving a dynamic range of 144 dB, sufficient to record the largest volcano-seismic events without saturation. The noise level at MBWH is particularly low, and it is sufficiently far away from the active flanks of the volcano (Fig. 1) to record events on different flanks without strong bias, making this the best station for further analysis. There is also a network of short-period seismometers; the signals from four of these are written to helicorders at MVO in real-time.

We also use satellite images of Montserrat to examine the timing of ash cloud development during the collapse event. The Caribbean region is imaged approximately once every 15 min by the Geostationary Operational Environmental Satellite-8 (GOES-8), which is situated in geostationary orbit at an altitude of ~36 000 km above the Americas (at 75°W). These data are collected and processed by the University of Hawaii for volcanic targets including SHV and are available online in near real-time (http://goes.higp.hawaii.edu/goes). GOES data have previously been used to study the ash clouds produced by activity at SHV during 1997–1999 (Rose and Mayberry, 2000).

Rainfall data in the form of daily totals are obtained from a network of rain gauges on Montserrat maintained by the Ministry of Agriculture of the Government of Montserrat. The rain gauge at Hope in west-central Montserrat (Fig. 1) is the source of the data presented here, since it was the closest rain gauge to the volcano at the time (~5.7 km from the SHV lava dome) and provided the most consistent dataset from 1999–2001. Rainfall data with higher temporal resolution were not available until January 2001 when a new rain gauge network was deployed (Matthews et al., 2002).

3. Activity prior to the 20 March 2000 dome collapse

Following the period of residual activity that began in March 1998 (Norton et al., 2002), dome growth recommenced at SHV sometime in mid to late-November 1999. An early view of the November 1999 (N99) dome is shown in Fig. 2a. From November 1999 until mid-February 2000, the focus of dome growth switched intermittently between the NW, SW and E sectors, with most of the activity concentrated in an eastern lobe directed towards the Tar River Valley (TRV; Fig. 1). This pattern of dome growth, involving the extrusion of an active lobe in a particular direction for several days or weeks before a switch to a different location, has been observed throughout the 1995–2003 SHV eruption (Watts et al., 2002). Throughout the November 1999–March 2000 phase of dome growth lava extrusion was proceeding at rates of ~2–3 m^3 s^{-1}, which is the approximate long-term average for the SHV eruption.

Between 18 February and 6 March 2000, activity was focused on the eastern lobe, directing semi-continuous rockfalls in a wide swath towards the TRV and extending the talus slope eastwards. Observations on 2 March confirmed that very little activity had occurred in the NW and SW sectors of the dome during this period. On 6 March, the focus of dome growth switched and a new lobe began to extrude southwards towards the crater rim of the 1995–1998 dome remnants (Fig. 2b). Rockfall activity on the eastern flank of the dome declined dramatically and instead talus began to bank up against the older dome material to the south.

In the days immediately prior to the 20 March collapse, extrusion continued in this southern sector and the summit height of the active southern lobe marginally exceeded the highest point on the 1995–1998 dome (the 940-m-high Northeast Buttress; Fig. 2b). On the morning of 20 March, accumulated talus from the active southern lobe had almost begun to overspill the southern crater rim near Galway's Peak. In addition, a prominent SE-directed spine had extruded at the rear of the southern lobe, indicating a slight switch in the direction of dome growth. A switch in extrusion direction was also suggested by rockfall trajectories, which had started to impinge once more on the eastern flank of the N99 dome.

The volume of the N99 dome was determined using photogrammetric techniques on two occasions between the resumption of dome growth in

mid-November 1999 and 20 March 2000. On 9 December 1999 the N99 dome volume was $\sim$5.2 Mm^3 and by 18 January 2000 this had increased to $\sim$15.4 Mm^3, indicating an average extrusion rate of $\sim$3 m^3 s^{-1} between those dates. Using extrusion rates of 2–3 m^3 s^{-1} to extrapolate dome growth through to 20 March, we arrive at an estimated volume of $\sim 29 \pm 3$ Mm^3 for the N99 dome immediately prior to the 20 March 2000 collapse.

Plots of seismic activity from shortly after the appearance of the N99 dome through the end of March 2000 are shown in Fig. 3. Prior to the major peak in rockfall energy on 20 March, rockfall activity was most vigorous in mid-February during emplacement of the eastern lobe of the N99 dome, which directed rockfalls and minor pyroclastic flows down the TRV. Thereafter, rockfall activity subsided as the southern lobe developed and rockfall runout distances diminished, and remained low until 20 March (Fig. 3). None of the other earthquake types exhibited any recognizable short-term precursory trends in the lead-up to the 20 March collapse, including hybrid earthquakes (Fig. 3), in contrast to SHV dome collapses in the 1995–1998 phase of dome growth (Table 1). On many occasions during phase 1 (e.g. 25 June 1997) precursory hybrid earthquake swarms gave sufficient warning of an impending collapse to allow an evacuation of areas in the path of potential dome-collapse pyroclastic flows before the event occurred (Voight et al., 1998). This lack of precursory short-term seismic activity suggests a lack of significant pres-

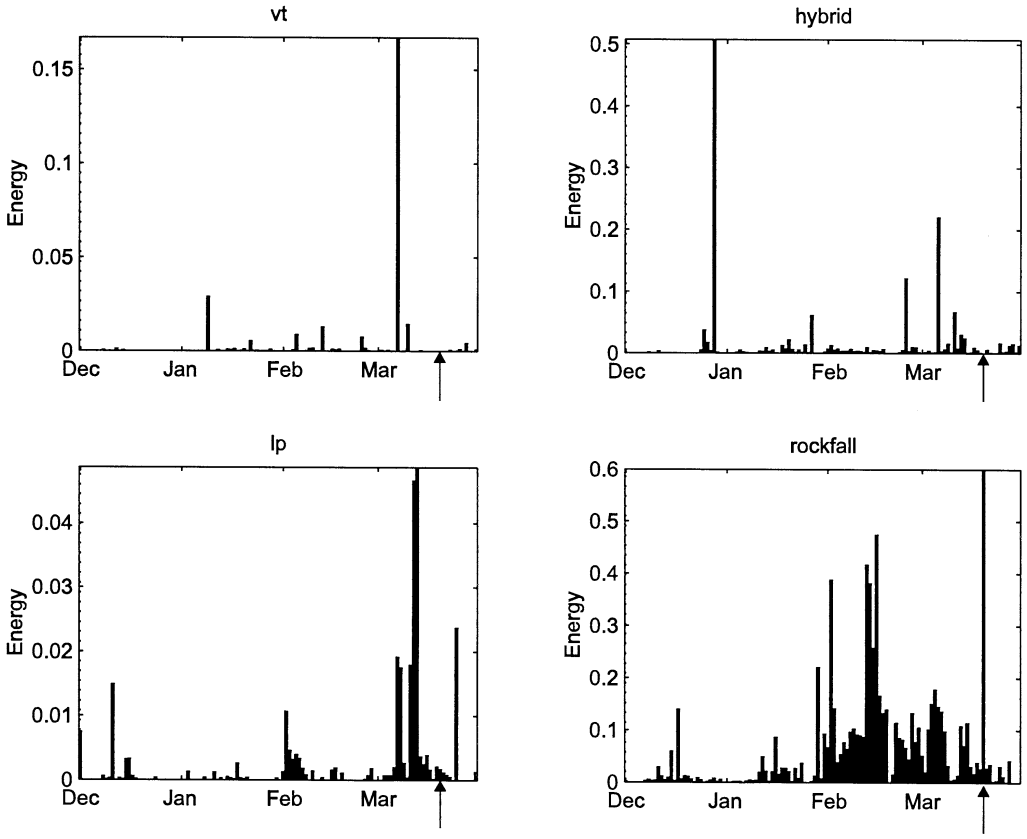

Fig. 3. Cumulative energy per day for different volcanic earthquakes (volcano-tectonic (vt), long-period (lp), hybrid and rockfall) recorded on the Windy Hill broadband seismometer (MBWH) for the period 1 December 1999 to 31 March 2000. Tick marks on the horizontal axis correspond to the first day of each month and 20 March 2000 is indicated by an arrow. The large spike in rockfall energy on 20 March actually exceeds 5. Note the lack of short-term precursory hybrid earthquake activity prior to the collapse.

surization in the conduit prior to the 20 March 2000 collapse, and we therefore conclude that the collapse was initiated by processes other than a fluctuating extrusion rate.

The most significant event to occur prior to the collapse on 20 March 2000 was not of volcanic origin. Around 20 minutes before the first seismic activity that heralded the collapse, an intense rainstorm developed over Montserrat. This rainfall event eventually produced the highest daily rainfall total of the 2000–2001 period at the Hope rain gauge (77 mm), and the second highest total recorded between January 1999 and September 2001 (Fig. 4). The highest daily rainfall total of the 1999–2001 period at Hope was recorded during the passage of Hurricane Jose to the north of Montserrat on 21 October 1999 (Fig. 4), when no active dome growth was occurring. The third largest amount of rain fell on 29–30 July 2001 when the next major dome collapse ensued (Matthews et al., 2002). Significant precipitation (associated with Hurricane Lenny) also occurred from 17 to 22 November 1999 during a gap in the daily rainfall record (Fig. 4), but the N99 lava dome was either absent or of negligible size at this time (although small explosions were reported; MVO, unpublished data, 1999). The only other noteworthy rainfall during a data gap at Hope fell on 17–18 December 2000 (Fig. 4), but no significant activity was noted at SHV and contemporaneous data from a rain gauge in the northern Centre Hills (Fig. 1) indicate that the rainfall was most likely spread over the two days (hence daily totals were probably not exceptional).

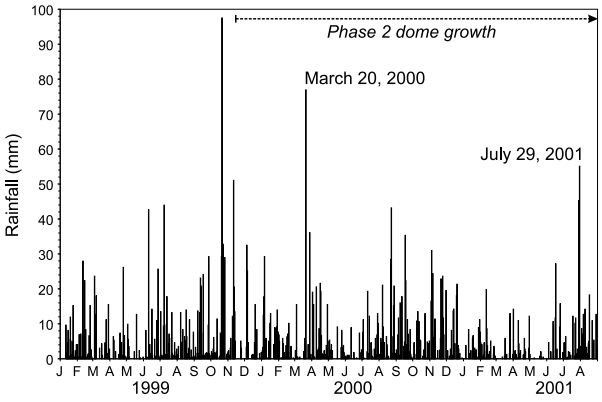

Fig. 4. Daily rainfall totals at the Hope rain gauge (Fig. 1) for 1 January 1999–31 August 2001. Tick marks on the horizontal axis correspond to the first day of each month. Breaks in the record indicate days on which no rain fell, days with negligible rainfall or days on which daily rainfall totals were not determined (data gaps). The latter account for 54 days in this time window. Most data gaps are 1–3 days in duration, with the longest spanning 11 days (1–11 January 1999). The amount of rain stored in the gauge following a data gap records the cumulative rainfall total for the data gap. The only data gaps with significant cumulative rainfall (>30 mm) occurred from 17–22 November 1999 (263 mm in 6 days) and from 17–18 December 2000 (49 mm in 2 days). Phase 2 of active dome growth at SHV is also indicated.

4. The 20 March 2000 dome collapse event

4.1. Field observations

Heavy rain began falling at Gerald's Heliport, ~10 km north of the volcano (Fig. 1) at 15:11 h (all times are local; UTC-4 hours). At 15:37 h an emergent seismic signal was recorded at MVO that increased markedly at 15:48 h (Fig. 5), and at ~16:15 h observers at Jack Boy Hill (Fig. 1) saw pyroclastic flows in the TRV. The ash plumes above these initial flows were not very convective and the flows were separated by gaps of ~5 min, a periodicity that is also evident in seismic data (Fig. 5). The runout distance of these flows was estimated to be 1–2 km down-valley from the lava dome, with occasional larger flows reaching the Tar River Delta (TRD; Fig. 1). The TRD is comprised of accumulated pyroclastic flow and mudflow deposits from the current eruption.

This rhythmic activity continued for around 2 hours until ~18:00 h when activity increased with higher-velocity pyroclastic flows rapidly reaching the TRD (Fig. 5). Some of these flows entered the sea at the edge of the TRD, producing small phreatic and/or phreatomagmatic explosions similar to those observed during previous dome collapses (e.g. Cole et al., 1998). The flows with highest velocity produced surge clouds that appeared to travel eastwards across the sea to at least 1 km offshore of the TRD (based on the geometry of observation position and coastline). In the initial burst of these flows, small lightning flashes were evident and their associated ash

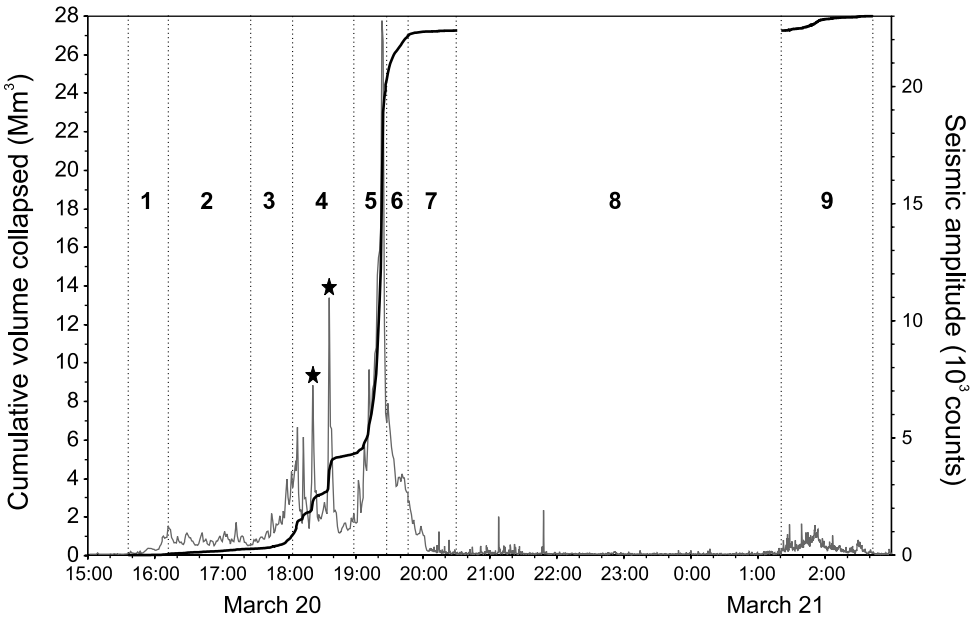

Fig. 5. RMS seismic amplitude data in 1-min bins recorded during the entire 20–21 March 2000 dome collapse by the broadband seismometer MBWH on Windy Hill (gray line), with a plot of cumulative seismic amplitude squared superimposed (black line) as a proxy for collapsed volume. Collapse stages (see Table 1) are delineated (dotted lines) and numbered. Stars indicate the signals associated with large pyroclastic flows at 18:21 and 18:36 h. See text for discussion.

plumes rose rapidly and near-vertically into the low meteorological cloud deck. Light ashfall began to drift eastwards indicating that a high-level plume had risen above the low-level easterly winds and was subjected to westerly winds at higher altitude. A constant, dull roaring sound seemed to be sourced from the eastern coastline and was attributed to the boiling of seawater in contact with fresh pyroclastic flow deposits.

Peak activity occurred at around 19:20 h (Fig. 5), when a very high-velocity pyroclastic flow entered the sea with accompanying flashes of lightning within the flow. The associated surge cloud spread rapidly eastwards across the sea to a distance of at least 1.5 km offshore of the TRD. Almost immediately thereafter, large glowing blocks were seen detaching from the eastern face of the remaining lava dome. Within a minute of this event, a spray of glowing ballistic blocks was ejected several hundred meters above the dome towards the east and/or northern flanks of the volcano, assumed to be the result of an explosion from the unroofed conduit area. Independent witnesses in the Old Towne area (Fig. 1) later reported seeing several small explosive events (directing ballistics to the south) from the summit area at this time. Intense thunder and lightning swiftly followed this explosive phase and ashfall occurred across northern Montserrat. Near-continuous dull glowing was observed at ~19:35 h around the main crater area and a strong odor of chlorine was evident in the atmosphere. Thunder and lightning gradually waned over the next 10 min.

The rainfall that had begun at Gerald's at 15:11 h continued intermittently until 07:37 h on 21 March, totalling 67.5 mm. Rainfall intensity at MVO was highest at the start of the event and gradually waned thereafter. Although conditions on the volcano at the time are not known, the summit of the dome was covered by dense meteorological cloud throughout the collapse, indicating that rainfall was almost certainly occurring. This is also supported by the observation of lahars and lahar deposits in channels on several flanks of the volcano during and after the collapse, including White's Ghaut, Tuitt's Ghaut, Fort Ghaut and the Belham Valley (Fig. 1).

4.2. Seismic data

Broadband seismic amplitude data recorded during the 20 March 2000 collapse are shown in Fig. 5. It is possible that the signal observed at 15:37 h was entirely due to lahars induced by heavy rain. Further intensification of the signal at 16:03 h suggested pyroclastic flow activity in the TRV and observations from Jack Boy Hill at 16:15 h confirmed this. From ~16:10 to 17:30 h seismicity was relatively constant (Fig. 5), then between 17:30 and 18:36 h seismic amplitude escalated by an order of magnitude. Pyroclastic surges extending offshore far beyond the edge of the TRD were observed corresponding to strong seismic signals at 18:21 and 18:36 h (Fig. 5). MVO's MJHT (Jack Boy Hill) seismometer, the least sensitive instrument on the short-period network being written to a helicorder, saturated briefly during this phase.

There then followed a brief repose until ~19:00 h after which a rapid escalation again occurred (Fig. 5). The largest seismic signal of the entire collapse sequence was recorded at 19:23 h corresponding to the field observations of ejected glowing ballistics. All short-period seismometers were saturated at this time. Spectral analysis of broadband seismic data showed that the dominant frequency during the most intense part of the collapse was ~ 2 Hz, typical of volcanic tremor. Seismicity then rapidly declined in a sequence of steps and had returned to background levels by 20:30 h (Fig. 5). The ensuing repose period was interrupted by a further collapse phase between 01:20 and 02:30 h on 21 March, which was similar in intensity to the 16:10–17:30 h phase on 20 March (Fig. 5).

Boulder-laden lahars over the Belham Bridge (across the Belham River south of Salem; Fig. 1) were first reported at 19:40 h on 20 March but probably began as early as 16:00 h. Unfortunately, the pyroclastic flow signals recorded during the collapse completely masked any lahar signals that may have otherwise been recorded by the seismic network.

The seismic data in Fig. 5 show a distinct ~5-min periodicity throughout the collapse that was also discernible in the field as a periodicity in the occurrence of large pyroclastic flows in the TRV. Assuming that each visible peak in the seismic data corresponds to an individual pyroclastic flow, or to a pyroclastic flow directly preceding or following an explosion, the data suggest that at least 38–41 pyroclastic flows were generated during the collapse, although these flows span two orders of magnitude in energy (Fig. 5). The piecemeal nature of the collapse event and the emergent trend in seismic energy suggest that the collapse was not caused by a catastrophic failure of the dome, which would have released a large volume of material in a shorter period of time. This would have produced a different trend in the seismic data, with higher initial amplitudes followed by a gradual decline in energy (e.g. the 3 July 1998 collapse; Norton et al., 2002). Instead, the 20 March 2000 collapse involved progressive degradation of the dome by pyroclastic flows with increasing velocity and runout distance, which gradually unroofed the hot, relatively gas-rich dome interior and conduit and ultimately precipitated the climactic explosions and the highest velocity surges/flows. A similar progression of events was recorded during the 17 September 1996 collapse (Table 1), which also culminated in an explosive eruption (Robertson et al., 1998).

4.3. GOES satellite observations

Data from GOES-8 offer some insights into activity preceding and during the 20 March 2000 event, and into the movement of the associated ash cloud in the hours following the collapse (Fig. 6). Examination of GOES imagery collected on 20 March indicates the first appearance of an ash plume over Montserrat at around 18:15 h local time. Subsequent images show the appearance of two pulses of ash drifting ~ESE from the island at around 18:45 h. Three such pulses are visible in an image at 19:15 h, also drifting ~ESE (Fig. 6a). These discrete ash clouds are interpreted as the products of either strong ash venting and/or small explosive events, or ash plumes lofted above larger pyroclastic flows, and may correlate with the seismic amplitude spikes observed in the build-up to the climactic explosions (Fig. 5). Measurements from the image sug-

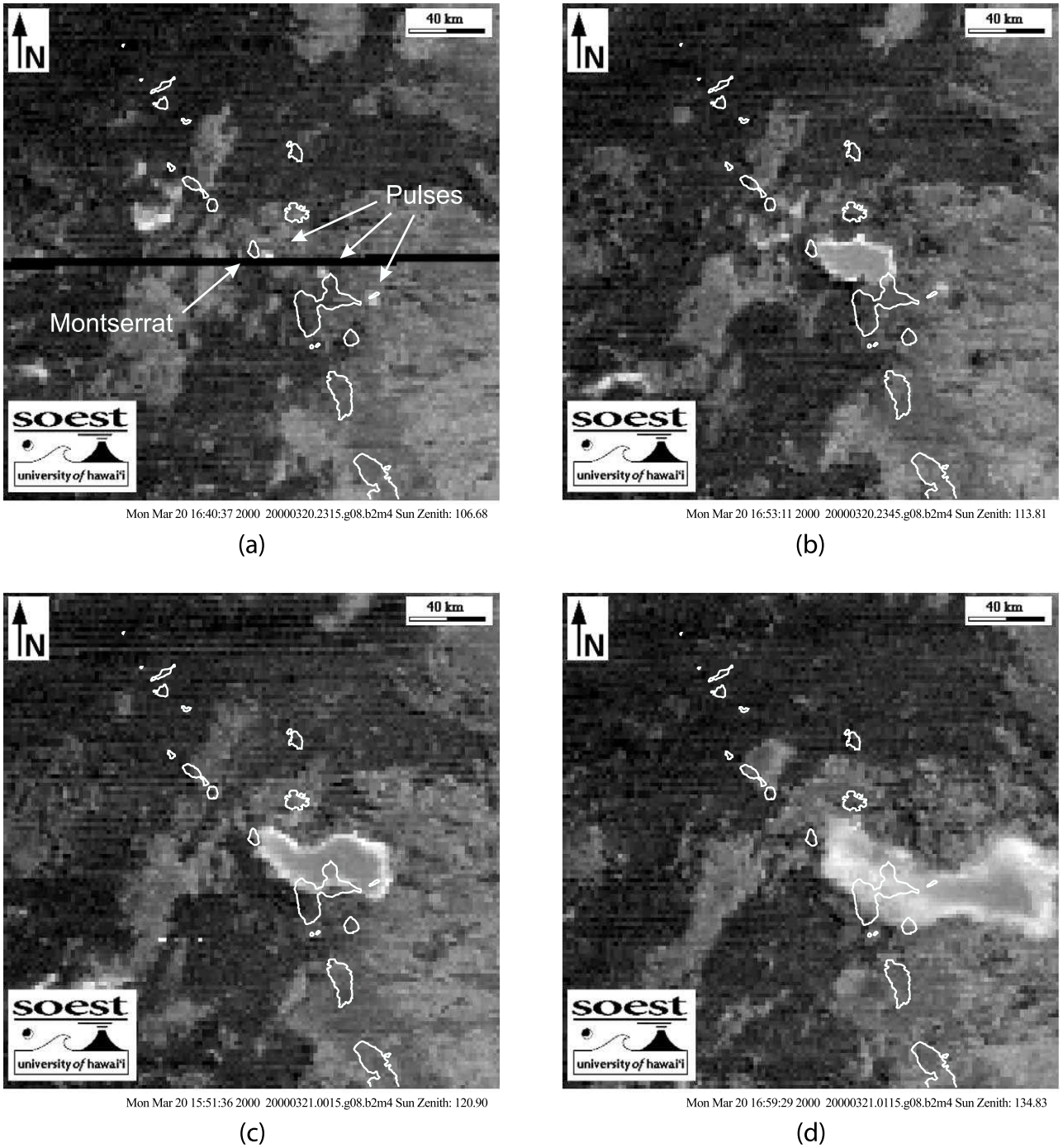

Fig. 6. GOES images showing the development of the ash clouds associated with the 20 March 2000 collapse. These images were obtained from the Hawai′i Institute of Geophysics and Planetology (University of Hawai′i) Hotspot Monitoring website (see text for URL) and involve a combination of Band 2 and Band 4 GOES Imager data. (a) Three discrete ash clouds or pulses visible at 17:15 h local time. There is a data gap across the middle of the image. (b) Emergence of main eruption plume at 19:45 h, note N–S oriented kink and single remaining pulse to ESE. (c) Wave-shaped plume spreading ~ESE at 20:15 h, over N and E Guadeloupe. (d) Continued eastward spreading of dense portion of plume at 21:15 h.

gest that the individual pulses are separated by a distance of ~30 km. Estimates of plume speed are difficult to ascertain without accurate knowledge of the altitude of the ash clouds, but according to NOAA (Satellite Analysis Branch) wind speeds were between 25 and 60 knots, increasing with altitude. A constant plume speed of 25 knots (12.9 m s^{-1}) would imply approximately 40 min between pulses, whilst a speed of 60 knots (30.8 m s^{-1}) would suggest a separation of ~16 min. A separation of ~16 min between the first two pulses correlates well with the two strong seismic signals at 18:21 and 18:36 h (Fig. 5), which coincided with high-velocity pyroclastic flows in the TRV.

At 19:32 h, ~9 min after the climactic explosions from the dome (Fig. 5), an eruption plume was clearly visible as it emerged through the meteorological cloud over Montserrat, and by 19:45 h a lobate ash cloud measuring approximately 30–40 km (E–W) by 20 km (N–S) had developed (Fig. 6b). One remaining pulse from an earlier pulse of activity was still located to the east, and the main plume, moving eastwards, was already impinging on Guadeloupe to the SE of Montserrat. Information from NOAA indicated that the plume observed at 19:45 h reached an altitude of at least 30 000 feet (~9 km), with lower-level ash drifting westwards.

The lobate ash cloud observed at 19:45 h displayed a N–S-oriented kink, which subsequently developed into a wave-like form drifting ~ESE evident at 20:15 h (Fig. 6c). This morphological change was probably due to wind shear acting on parts of the plume at different altitudes. By this time the cloud was covering a large part of northern and eastern Guadeloupe, where light ashfall was reported. The distal end of the cloud continued spreading eastwards and by 21:15 h it had dimensions of ~100–120 km by ~40 km. Also, at this time the cloud appeared to be splitting into two segments, a dense portion heading ~ESE and a smaller, more diffuse portion hanging over and to the SE of Montserrat (possibly evaporated seawater and lower level ash). The main cloud continued to spread towards the ~ESE and by 23:45 h it extended ~305 km from Montserrat and was ~120 km wide. Over the next few hours the cloud dispersed in the vicinity of Montserrat, with little ash evident in images after 02:46 h on 21 March despite the occurrence of further pyroclastic flow signals at around 01:30 h. We thus conclude that no major explosive activity was involved in the final stage of the collapse. However, the main cloud continued to drift over the Atlantic Ocean and by 08:45 h mid-level ash (at ~5 km altitude) was still detectable around 710 km east of SHV, with high-level ash (~10 km altitude) no longer apparent. Dense clouds over Montserrat at that time precluded the detection of any low-level ash over the island, but this was probably removed by overnight rain.

4.4. Post-collapse features and deposits

Inclement conditions in the days following the 20 March 2000 collapse, and the removal by rainfall of most of the deposits emplaced on land, prohibited a detailed assessment of the collapse products. However, several key observations were made that contribute to an analysis of the event.

Airborne investigations of the collapse scar reamed out during the activity on 20 March were conducted on 24 March during the first clear weather after the collapse. Observations indicated that ~95% of the N99 dome had been removed, thus amounting to a volume of 28 ± 3 Mm^3 (continued dome growth at extrusion rates of ~2–3 m^3 s^{-1} during the ~5-h main phase of the collapse would have added only ~0.04–0.05 Mm^3 of new lava; this is ignored in our volume estimate). Estimated volumes of other large dome collapses at SHV are given in Table 1 for comparison. We adopt a nominal 20 March 2000 collapse volume of 28 Mm^3 in the remainder of the paper.

Post-collapse observations confirmed that the block-and-ash deposits emplaced by pyroclastic flow activity had been entirely confined within the TRV to the east of the dome, with associated surge zones extending less than 1 km north and south of the TRV at their maximum extent. Deposition of block-and-ash flow (BAF) deposits on the TRD had enlarged this feature in a N–S direction, with some erosion of the delta where pyroclastic flows had entered the sea on its eastern

Fig. 7. A view of the Tar River delta (see Fig. 1) on 30 March 2000, looking ~WSW. Light gray block-and-ash flow deposits emplaced during the 20 March 2000 collapse drape most of the delta. Note the prominent trench across the delta (ET), eroded through older deposits during the collapse, extending from the base of the Tar River Valley approximately eastwards to the sea. The dark, lobate flow deposit immediately north of the trench was produced by post-20 March activity. Also indicated are a narrower trench eroded across the delta towards the ~SE (ST), and a similar trench (not as clear in this view) eroded towards the ~NE (NT). The summit of SHV is hidden by cloud in the center background.

margin (Fig. 7). The most significant change to the TRD resulting from the collapse was the erosion of three large trenches through the pre-existing deposits, extending to the shoreline, with the largest trench (cut directly across the central part of the TRD with an eastward trend) measuring 5–10 m deep by 50–80 m wide (Fig. 7). Two smaller trenches radiated away from the main channel where the TRV met the TRD. Although the erosive capacity of SHV pyroclastic flows has been previously noted (e.g. the 17 September 1996 flows; Cole et al., 1998), erosional channels had not been observed at this distance from the dome (i.e. on the TRD) in the aftermath of any previous SHV dome collapse, suggesting that the pyroclastic flows generated towards the climax of the 20 March 2000 event were exceptionally erosive (comparable erosive channels were also observed on the TRD following the 29 July 2001 dome collapse). The bulk of the collapse deposits were therefore emplaced offshore of the TRD, prohibiting an estimate of their volume, although a topographic survey of the TRD indicated that only ~10% of the estimated total collapse volume (i.e. ~3 Mm^3) had been emplaced on the subaerial part of the delta. Negligible deposition had occurred within the TRV between the dome and the TRD.

The 20 March 2000 BAF deposits that draped much of the TRD (Fig. 7) were laden with numerous large sub-angular clasts, some exceeding 2 m in diameter, protruding from the deposit surface. These clasts may have been partly responsible for the highly erosive nature of the pyroclastic flows, and the lack of fragmentation suggests that the clasts had low 'autoexplosivity' or excess pore pressures (Sato et al., 1992). However, brief observations did not reveal the deposits to be substantially different from BAF deposits emplaced by prior SHV dome collapses (e.g. Calder et al., 1999). Much of the TRD was also blanketed with a 10–15-cm-thick layer of fallout deposits produced by the interaction of pyroclastic flows and seawater, including abundant accretionary lapilli. No significant pumice fraction was found in the fallout deposits on Montserrat, nor in the ashfall retrieved and analyzed on Guadeloupe (Observatoire Volcanologique de la Soufrière de Guade-

loupe [OVSG], unpublished data, 2000), suggesting that even the climactic explosions of the 20 March 2000 event did not involve the eruption of significant quantities of volatile-rich magma. The ash was primarily composed of porphyritic andesite clasts and sub-angular to angular crystals (OVSG, unpublished data, 2000), suggesting that it was the product of fragmentation of the pre-existing N99 dome.

4.5. Post-collapse dome growth

Limited observations suggest that extrusion of the March 2000 dome began almost immediately following the 20 March 2000 collapse. New spines sighted over the conduit region in the collapse scar on 24 March confirmed that extrusion was ongoing, and the relatively short time span between the collapse and the reappearance of extruded lava indicates that the conduit was only reamed out to shallow levels by the 20 March explosive activity.

In keeping with typical patterns of post-collapse activity observed during the SHV eruption, estimated dome growth rates were slightly higher ($\sim$3–5 m^3 s^{-1}) following 20 March 2000 due to the removal of substantial conduit overburden (estimated at $\sim$4.5–6.25 MPa). Seismic activity was dominated by banded tremor, with bands typically lasting 2–3 h and occurring every 5–7 h between late March and 8 April. Tremor bands were at times visually correlated with ash venting from the volcano. Theoretical work on stick-slip conduit flow of compressible magma (e.g. Denlinger and Hoblitt, 1999) suggests that such banded tremor relates to short-term variations in magma extrusion rate.

Although explosions were observed during the paroxysmal phase of the 20 March 2000 collapse, and episodes of ash venting occurred sporadically after the event, no subsequent Vulcanian explosions were precipitated by the removal of almost the entire N99 dome. Vulcanian explosions, with eruption columns attaining altitudes of $>$15 km on occasions and often accompanied by pumice-rich column collapse pyroclastic flows, occurred after dome collapses of a smaller magnitude on 17 September 1996, 3 August 1997 and 21 September 1997 (Robertson et al., 1998; Druitt et al., 2002), continuing for several weeks in 1997. This implies that the magma in the post-20 March 2000 conduit was not particularly volatile-rich, at least not at shallow depths, and argues for a change in the degassing regime at SHV between phase 1 (closed-system degassing prior to explosive activity) and phase 2 (open-system) of dome growth (Edmonds et al., 2002).

5. Analysis of the broadband seismic record

In order to visualize the progression of the 20 March 2000 collapse in more detail we have performed an analysis of the broadband seismic record at MBWH (Windy Hill; Fig. 1) and calibrated the recorded seismic energy with the total collapsed volume of $\sim$28 Mm^3 (Table 2; Fig. 5). Our method is analogous to that of Brodscholl et al. (2000), who analyzed broadband seismic data recorded during the 22 November 1994 dome collapse at Merapi volcano, and whose work was based on a technique originally developed by Norris (1994). We use the square of seismic amplitude (effectively a measure of seismic energy) as a proxy for volume (A.D. Jolly, written commun., 2001).

Since we are using only one seismometer in this analysis, the technique assumes similar source areas and descent paths for the pyroclastic flows (Brodscholl et al., 2000). Our field observations indicate that this approach is valid for the 20 March 2000 collapse since all activity was sourced from the collapsing lava dome and pyroclastic currents were confined to the TRV (Fig. 1). Other potential sources of seismic energy, such as teleseismic events, microseismicity or lahars, can also be discounted since no teleseismic signals were recorded at any MVO seismometers during the collapse event, and the pyroclastic flow signals were large enough to easily overwhelm any other possible sources. A more detailed discussion of these and other issues relevant to the method is given by Brodscholl et al. (2000).

The broadband seismic record from MBWH and the cumulative collapsed volume are shown in Fig. 5. Data for each of the collapse stages

Table 2
Collapsed volume and discharge rate (inferred from broadband seismic data) for stages of the 20 March 2000 collapse

Stage	Local time	Collapsed volume (Mm^3)	Cumulative %	Discharge rate ($m^3\ s^{-1}$)	Activity
1	15:36–16:12	0.092	0.3	43	Emergent signal
2	16:12–17:27	0.233	1.2	52	Intermittent Pfs
3	17:27–18:05	0.927	4.5	407	Increased rate of collapse
4	18:05–19:00	4.045	18.9	1226	Fluctuating Pfs
5	19:00–19:26	19.151	87.3	12277	Paroxysm (largest Pfs, explosions)
6	19:26–19:46	2.550	96.4	2125	Waning activity
7	19:46–20:30	0.254	97.3	96	Waning activity
8	20:30–01:21	0	97.3	0	Little activity
9	01:21–02:44	0.747	100	150	Small resurgence

demarcated on Fig. 5 are tabulated in Table 2, including average discharge rates for each time period. The isolated spikes in seismic amplitude recorded during stage 8 (Fig. 5), probably the result of small rockfalls or lahars, are regarded as negligible and hence we assume zero discharge rate during this period (Table 2).

The data indicate that the paroxysmal phase of the collapse (19:00–19:26 h) removed by far the greatest proportion (~68% of the total collapse volume) of the N99 dome, amounting to ~19 Mm^3 at an average discharge rate of ~12 300 $m^3\ s^{-1}$ (Table 2). We can also use the calibrated seismic record to estimate the volume of lava removed by each individual pyroclastic flow, although these figures cannot be verified as much of the collapsed dome was emplaced offshore. As remarked earlier, if each visible peak in the seismic data corresponds to an individual flow, then approximately 38–41 pyroclastic flows can be identified in the seismic record between 15:36 and 20:30 h (Fig. 5). We note that the flow signals are superimposed on a persistent high-level background seismicity (Fig. 5), probably caused by near-continuous rockfalls which periodically merge to form larger pyroclastic flows. Using zero amplitude as a baseline gives an average flow volume (including the contribution from rockfalls) of 0.68–0.74 Mm^3, which is an order of magnitude larger than the average size of 44 nuées ardentes (0.06 Mm^3) generated during the 22 November 1994 dome collapse at Merapi (Brodscholl et al., 2000). However, the 20 March 2000 flows varied in energy by over two orders of magnitude (Fig. 5) and hence we have also calculated flow magnitudes for shorter time periods and individual events (Table 3).

The data in Table 3 show that the seismic signals recorded in the first ~10 min of the collapse (15:36–15:47 h) resulted from small flows (~300 m^3 per flow) that were most likely small rockfalls or lahars. In fact the average discharge rate (1.5 $m^3\ s^{-1}$) of these initial flows is at the lower end of the range of values recorded for rain-triggered lahars on Montserrat in 1998 (0.5–282 $m^3\ s^{-1}$; MVO unpublished data, 1998). In view of the heavy rainfall that commenced shortly before the collapse began, it is quite likely that these precursory flows were indeed lahars in the TRV, possibly resulting from erosion of dome talus.

Following this initial activity the rate of collapse increased rapidly, and during stage 2 the size of the average pyroclastic flow was ~0.02

Table 3
Average volume of 20 March 2000 pyroclastic flows (Pfs) inferred from seismic data for various time intervals during the collapse

Stage	Local time	No. of Pfs	Average Pf volume (Mm^3)
1	15:36–15:47	3	0.0003
	15:36–16:12	5	0.018
2	16:12–17:27	12	0.019
3	17:27–18:05	9	0.103
4	18:05–19:00	7	0.578
	18:18–18:26	1	0.859
	18:34–18:45	1	1.791
5	19:00–19:26	5	3.830
	19:13–19:27	1	17.667

Mm^3 (Table 3). The average discharge rate during this period (52 m^3 s^{-1}; Table 2) is still within the range of values for lahars quoted above, but field observations at this time noted the presence of weakly convecting ash plumes suggesting pyroclastic flows. After stage 2 the rate of collapse underwent another substantial increase (stage 3; Tables 2 and 3) and during stage 4 two large pyroclastic flows produced significant ash clouds (Fig. 5). For the flow that peaked at 18:21 h we estimate a volume of ~0.86 Mm^3 (Table 3) and a discharge rate of ~1790 m^3 s^{-1}. The larger flow that peaked at 18:36 h was around twice the magnitude of the 18:21 h event (Table 3), with an estimated discharge rate of ~2710 m^3 s^{-1}. At the climax of the collapse between 19:13 and 19:27 h an estimated ~17.7 Mm^3 of the N99 dome was shed (Table 3) at a rate of ~21 030 m^3 s^{-1}. Field observations confirm that the largest flows (and their associated pyroclastic surges) were the most mobile and travelled furthest from the collapsing dome. This is also generally evident from previously published data on Montserrat pyroclastic flows (Calder et al., 1999) and was also suspected for the 22 November 1994 flows at Merapi (Abdurachman et al., 2000). The progressive removal of the outer layers of the dome during the collapse would gradually expose the hotter, more gas-rich core, and produce pyroclastic flows with increasing velocity and runout distance.

The estimated volumes and discharge rates of the 20 March 2000 pyroclastic flows are compared with values for other dome collapses at SHV and at dome-forming volcanoes elsewhere. Calder et al. (1999) give volumes ranging from 0.15 to 14 Mm^3 for SHV dome collapse flows in 1996–1997 (also see Table 1), determined by field mapping of deposits and analysis of digital elevation maps. Assuming that the volumes in Calder et al. (1999) refer to individual pyroclastic flows, the data are similar in magnitude to our estimates of flow volumes for stages 3–5 of the 20 March 2000 collapse (Table 3), suggesting that our methodology produces reasonable results. Our data therefore indicate that individual 20 March 2000 flows were not substantially different in volume from previous SHV dome collapse flows, with the possible exception of the largest flow at the peak of the collapse (Table 3). Individual flow volume data for SHV dome collapses in 1998–2003 are not currently available for comparison and flow discharge rates are yet to be determined for any other SHV dome collapse.

Data concerning lava dome collapses at other volcanoes are also rather limited. The largest collapse event of the 1991–1995 Unzen (Japan) eruption occurred on 15 September 1991 and involved ~4 Mm^3 of lava dome and older rocks in four separate pyroclastic flows (Nakada, 2000). Hence these flows were comparable to those in stages 4 and 5 of the 20 March 2000 collapse at SHV (Table 3). From the analysis of the first 90 min of the 22 November 1994 dome collapse at Merapi by Brodscholl et al. (2000), we obtain an average discharge rate of ~306 m^3 s^{-1}. However, the largest individual dome slice that collapsed in that period produced a short-term discharge rate of ~1440 m^3 s^{-1} (Brodscholl et al., 2000). The Merapi flows were thus, on average, comparable to those in the earlier stages (2–3) of the 20 March 2000 collapse at SHV, though the largest Merapi event was similar in magnitude to the stage 4 flows on 20 March (Table 2). Hence, although available data are limited, the volumes and discharge rates of the largest dome collapse pyroclastic flows at SHV on 20 March 2000 exceed those documented for other recent dome-forming eruptions by up to an order of magnitude.

6. A rainfall-induced dome collapse?

In view of the lack of recognizable geophysical precursors to the 20 March 2000 collapse, we implicate the major rainfall event that coincided with the start of the collapse (Fig. 4) in its initiation and potentially in its prolongation. A similar scenario has been proposed for the 29 July 2001 collapse on Montserrat, which removed ~45 Mm^3 of the March 2000 dome (Table 1) and for which real-time rainfall intensity data are available (Matthews et al., 2002). We note that a combination of extenuating factors, in which the intense rain played a major role, may also have been involved, such as a change in the direction

of dome growth shortly before the collapse that destabilized the dome. Charts of daily rainfall for 1999–2001 (Fig. 4) clearly demonstrate the exceptional magnitude of the rainfall totals for 20 March 2000 and 29 July 2001, which were the highest recorded in the 21-month period of active dome growth that commenced in November 1999. Actual rainfall intensities on 20 March 2000 are not known although visual observations on the day confirm exceptionally heavy rain.

Although the Hope rain gauge that supplied the rainfall data shown in Fig. 4 is ~5.7 km northwest of SHV (Fig. 1), the observation of large mudflows on several flanks of the volcano during the collapse is convincing evidence that rainfall was at least as intense over SHV as it was elsewhere on Montserrat. This would also be expected as the volcano's summit is the highest point on the island and hence the most likely location of convective rainfall. According to Matthews et al. (2002), the 20 March 2000 rainfall event was most likely 'due to a short-lived and highly localized convective weather system over Montserrat that was essentially unpredictable', and not part of an organized weather system or 'tropical wave' of the type that initiated the 29 July 2001 collapse, which could have been tracked by satellite. Based on the chronology of events on 20 March 2000, it would therefore be difficult to provide much more than ~30 min advance warning of a rainfall-induced dome failure precipitated by a 'freak' storm of this kind, even if a network of rain gauges monitoring rainfall intensity in real-time was available. However, such a network could provide a useful tool for monitoring a rainfall-induced collapse following its initiation (e.g. Matthews et al., 2002).

6.1. Existing evidence for rainfall-triggered volcanic activity

The link between rainfall and volcanic activity is a frequently debated and contentious issue, but not without considerable circumstantial evidence. Care must be taken when classifying rainfall-induced (or other externally forced) 'events' on a volcano as *volcanic* activity, which in the strictest sense implies the action of internal, magmatic processes (see Neuberg (2000) for a discussion), though here we classify any potentially hazardous volcanic phenomenon as volcanic activity. There are well-documented links between heavy rainfall and mass-movements at quiescent volcanoes, a prominent recent example being the devastating debris avalanche at Casita Volcano, Nicaragua, during the passage of Hurricane Mitch in 1998 (Kerle and van Wyk de Vries, 2001), but here we focus our discussion on active volcanoes.

Dome-forming volcanoes seem especially susceptible to forcing by rainfall events, particularly in the tropics where rainfall can be intense, prolonged and seasonal. Along with the 20 March 2000 and 29 July 2001 collapses of the SHV lava dome (Matthews et al., 2002), Norton et al. (2002) also link the 3 July 1998 SHV dome collapse with intense rainfall prior to and during the event, perhaps in conjunction with weakening of the dome interior through hydrothermal activity. Elsewhere in the Lesser Antilles and several decades earlier, Perret (1937) described the effects of rainfall on the lava dome at Mt. Pelée, in his classic account of the 1929–1932 eruption on Martinique. On 17–18 April 1930, tropical downpours gave rise to what Perret (1937) described as 'steaming nuées ardentes' which continued 'from 4:00 in the afternoon to well into the night' (Perret, 1937). If the phenomena Perret observed were genuine pyroclastic flows rather than hot lahars producing steam, this suggests a sustained collapse possibly triggered by rainfall. In Perret's own words: 'Water, reacting with the hot dome, had forced it to disgorge some of its lava, forming an avalanche of steam and hot rock, imposing in magnitude, but not of course a primary volcanic manifestation' (Perret, 1937, p. 51). He also documents 'hot blasts' from the lava dome, following bouts of heavy rainfall by periods of between 15 min and 1.5 h (Perret, 1937, p. 97), and remarks that large lava blocks showed a 'stronger tendency to fissure and break up on the side predominantly exposed to rain and sun', due, he surmises, to rapid temperature changes (Perret, 1937, p. 50).

The last century of dome-building activity at Merapi has produced many reports of increased activity contemporaneous with heavy rains, particularly in recent years when observations have

become more frequent and better recorded (Mastin, 1994; Voight et al., 2000a; Ratdomopurbo and Poupinet, 2000). Heavy rains are inferred to have triggered phreatic explosions during activity in 1904, and may also have generated dome-collapse nuées ardentes in October 1920 (Voight et al., 2000a and references therein). Devastating pyroclastic flows in December 1930, which removed an older dome complex along with newer growth and took 1369 lives, were preceded by heavy rains two days earlier, and a sequence of 119 nuées in November 1961 may also have been induced by rainfall (Voight et al., 2000a). 'Intensive sliding' typically occurs at Merapi in the rainy season (beginning in November) and can remove 20–30% of the dome's volume (SEAN, 1984; it is not clear from the report whether the 'intensive sliding' involves pyroclastic flows or just lahars), although the large 22 November 1994 dome collapse was not associated with rainfall (GVN, 1994b). Coincidences between strong rains and dome-collapse episodes were also reported in October 1986 (when no seismic precursors were distinguished; Voight et al., 2000a); pyroclastic flows followed heavy or prolonged rains in August and November 1992 (GVN, 1992a, b) and February 1993 (GVN, 1993a); and an explosion and pyroclastic flow occurred after heavy rains in January 1996 (GVN, 1997). Increased volcanic tremor and gas emissions have also been observed after the beginning of the rainy season at Merapi (GVN, 1994a).

During the 1991–1995 Unzen eruption, rainfall allegedly triggered dome collapses and pyroclastic flows, with heavier rains increasing the likelihood of collapse (Yamasato et al., 1997). However, collapse episodes and precipitation did not correlate on all occasions. Yamasato et al. (1997) note that rainfall-induced dome collapses at Unzen were initiated on fresh, uncooled lava, and contend that rapid cooling of the hot lava by rainwater cracked the rock and led to failure.

Although there is no direct evidence for it on Montserrat, hydrovolcanic or phreatic activity has also been associated with rainfall at active and quiescent volcanoes. The March 1979 eruption of Karkar Volcano (Papua New Guinea), which took the lives of two volcanologists who were observing the volcano, involved laterally-directed explosions believed to have been generated by vaporization of groundwater in contact with hot rocks (McKee et al., 1981). These explosions were part of a sequence of explosive events between January and August 1979 that showed a good correlation with periods of rainfall, and which were attributed to increased influxes of meteoric water to the system that perturbed the usual steady-state vaporization process (McKee et al., 1981). Similar reasoning could explain a series of ~28 gas explosions from the Mount St. Helens (USA) lava dome between August 1989 and June 1991, which erupted no juvenile material but still hurled meter-scale ballistics up to a kilometer from the vent and generated 5-km-high ash plumes (Mastin, 1993, 1994). Most of the explosive events occurred within hours to 3 days after storms, and Mastin (1993, 1994) speculated that pressurized gases beneath the dome may have been released through cooling fractures or after rainfall-induced avalanches removed portions of the edifice. Evidence can also be found for increased explosive activity in the rainy season at the Santiaguito lava dome, Guatemala (GVN, 1990), and Guagua Pichincha, Ecuador (GVN, 1993b).

6.2. *A model for rainfall-induced dome collapse*

An important yet unresolved question is the mechanism by which rainfall could initiate or sustain volcanic activity. In the case of lava domes there are several possible processes that may be significant, including: (1) mechanical erosion by water that destabilizes critically poised segments of the dome or exposes pressurized gases (e.g. Mastin, 1993, 1994); (2) generation of destabilizing phreatic explosions as water percolates into the hot dome interior; (3) rapid cooling of hot lava causing it to fragment and/or release pressurized gases (e.g. Mastin, 1993, 1994; Yamasato et al., 1997); (4) the action of pressurized water or steam on potential failure surfaces within the dome (e.g. Voight and Elsworth, 2000); or some combination of these processes.

Available data for the 20 March 2000 lava dome collapse at SHV provide few clues as to

the potential trigger mechanism. The seismic record was dominated by pyroclastic flow signals and hence no short-lived, impulsive events (characteristic of explosions) could be recognized. A potentially significant feature of the event is that it began with relatively low-energy lahar-type signals (Table 2) in the TRV before the rapid escalation to pyroclastic flows, which suggests that erosion of the dome talus by intense rainfall was taking place. Rainfall intensity data for the 29 July 2001 collapse (Matthews et al., 2002) demonstrate the apparent rapid response of the lava dome to the most intense bouts of rainfall, which could support mechanism (1) and/or (3). On 20 March 2000 erosion could have destabilized the critically poised eastern face of the dome, and coupled with a more easterly growth direction (suggested by the observation of spines on 20 March prior to the collapse) may have initiated the collapse. However, any of the other aforementioned processes may also have played a role. In our opinion a shift in dome growth direction alone would not have generated such a sustained collapse, and we rule this out as a trigger for the 20 March 2000 event.

Although detailed modeling of the effects of rainfall on a hot lava dome is beyond the scope of this paper, we have used a simple energy balance model to address the feasibility of a rainfall-induced dome collapse by comparing the energy required to vaporize rainwater falling onto the dome at various intensities with the sensible heat flux from the dome. The N99 SHV lava dome is conceptualized as a circular cone with a volume of 29 Mm^3 and a height of 200 m, which implies a basal radius (r) of $\sim$372 m, a slant height (s) of $\sim$422 m and a surface area ($=\pi rs$) of $\sim$0.494 km^2.

Using rainfall intensities of 0.01–2.0 mm min^{-1}, with the upper bound analogous to the peak intensities recorded during the 29 July 2001 collapse (Matthews et al., 2002), implies a mass flux of water of $\sim$5–1000 tons min^{-1} onto the surface area of the dome. Heating this water from the ambient temperature (T_{air}; assumed to be 25°C) to 100°C and vaporizing it would require an energy flux of $\sim$0.013–2.5 terajoules (TJ) min^{-1} (using a specific heat capacity of water of 4.184 J g^{-1} K^{-1} and a latent heat of evaporation of 2260 J g^{-1}, and neglecting any effects of wind speed and water vapor pressure for simplicity). To estimate the sensible heat flux from the lava dome (with surface temperature T_{dome}), we use the following equations for convective heat loss (Q_{conv}) and heat advected by the gas phase (Q_{gas}) from Oppenheimer (1991) and Harris et al. (1999):

$$Q_{conv} = 0.14 S k_{air}^3 \sqrt{(g\alpha_{air}\rho_{air}/\nu_{air}\kappa_{air})}\,\sqrt[3]{(\Delta T)^4} \quad (1)$$

$$Q_{gas} = F_{gas} C_g \Delta T_{gas} + F_{H_2O} L_v \quad (2)$$

where S is the dome surface area, $\Delta T = T_{dome} - T_{air}$, g is acceleration due to gravity (9.8 m s^{-2}), k_{air}, α_{air}, ρ_{air}, ν_{air}, and κ_{air} are the thermal conductivity, cubic expansivity, density, kinematic viscosity and thermal diffusivity of air at the mean temperature $T_{air}+\Delta T/2$ (derived from tables in Kays and Crawford (1980)), F_{gas} is the total gas flux, C_g is the specific heat capacity of the gas (set at 1.6 J g^{-1} K^{-1}), ΔT_{gas} is the difference between magmatic temperature (800°C) and T_{air}, F_{H_2O} is the water vapor flux and L_v is the latent heat of condensation (2260 J g^{-1}). Using gas compositions determined by Hammouya et al. (1998) and an SO_2 flux of 3.1 kg s^{-1} (270 tons day^{-1}) measured by correlation spectrometry (COSPEC) on 20 March 2000 (MVO, unpublished data, 2000), F_{gas} and F_{H_2O} are set to 217 kg s^{-1} and 196 kg s^{-1}, respectively. T_{dome} is a difficult parameter to constrain, since it is likely to vary considerably over the dome surface. Much of the SHV dome is typically covered by a relatively cool carapace, with hotter material present where it is exposed in cracks, generated by fragmentation during rockfalls, or heated by hot gases liberated from the interior. In the region of active dome growth hotter, relatively fresh lava will also be present at or near the surface of the dome, raising its temperature to near-magmatic values. Furthermore, the area occupied by each of these features will vary dynamically as the dome evolves; a larger dome may have a greater proportion of cooler talus on its flanks for example. Hence assigning a representative T_{dome} is problematic and any interaction of the dome with rainwater is likely to vary across its surface.

For values of T_{dome} ranging from 300–1100 K (~27–827°C), derived values of $Q_{conv}+Q_{gas}$ are ~0.04–0.25 TJ min^{-1}. Balancing this heat flux with the energy required to vaporize falling rainwater indicates that rainfall intensities in excess of 0.2 mm min^{-1} are sufficient to allow liquid water to reach the dome, irrespective of its surface temperature. If Q_{gas} is increased by raising the assumed SO_2 flux to an extreme value of 23 kg s^{-1} (~2000 t d^{-1}; well above the long-term SHV average of ~500 t d^{-1}), the range of $Q_{conv}+Q_{gas}$ becomes ~0.32–0.53 TJ min^{-1} and rainfall intensities higher than 0.42 mm min^{-1} are required to overwhelm the vaporization process. Clearly, once rainwater comes into contact with the hot surface of the lava dome, evaporation will also take place at a rate dependent on the dome temperature, rainfall intensity, wind speed and local water vapor pressure, with accumulating water more likely at higher rainfall rates. Whilst not attempting to model this process, we contend that sustained rainfall at above a threshold intensity would be required to allow continuous interaction between water and dome rock. This would lead to erosion of, and/or percolation of water into, the lava dome, with the latter process potentially leading to phreatic explosions or the generation of pressurized steam, and fragmentation of the dome surface. Data collected during the 29 July 2001 collapse (Matthews et al., 2002) indicate that the collapse was not initiated until rainfall became sustained at high intensity for periods >1 h. The data in Fig. 4 also point to the importance of sustained rainfall (i.e. high total amounts) in triggering dome collapses on Montserrat.

We therefore propose a simple model for the 20 March 2000 dome collapse at SHV. In the early stages of the collapse, mechanical erosion of dome talus, producing lahars in the TRV, was probably important. This would have exposed hotter material beneath the dome surface and may also have destabilized segments of the dome's eastern flank. Erosion of cooler talus on the lower flanks of the dome may have continued throughout the collapse, although the volume removed in this way was probably insignificant relative to the volume removed and/or eroded by later pyroclastic flows. As rainfall continued, interaction between water and hot lava became more significant. Cooling and fragmentation of hot lava in contact with water released pressurized gases and generated pyroclastic flows, with this process sustained by continuous rainfall. As the collapse progressed, the hotter, gas-rich core of the dome became increasingly exposed, and the heavily fractured interiors of individual dome lobes were shed in larger pyroclastic flows, possibly generating small explosive events. At this stage, the release of pressurized gases from the core of the dome may have been the main driving force behind the collapse, with the rainfall now playing a subordinate role. Finally, the volatile-rich magma in the conduit region was exposed, triggering an explosion and the highest-velocity pyroclastic flows at the climax of the collapse.

7. Discussion

There is therefore a growing body of evidence linking rainfall with various types of volcanic activity, although, with the exception of the 29 July 2001 collapse of the SHV dome (Matthews et al., 2002), much of it is based on statistical correlations or simple coincidences. Such activity is hazardous as it is usually unpredictable. Although it may be possible to forecast significant rainfall up to several days in advance using satellite imagery, a better understanding of the relationship between rainfall (amount and intensity) and volcanic activity is required before such forecasts can be used to pre-empt potential volcanic hazards. On Montserrat heavy rain is commonplace during the June–December rainy season and it typically triggers mudflows, but sustained rainfall-induced dome collapses are a rare occurrence. Evidence from the 20 March 2000 and 29 July 2001 collapses implies that rainfall must be both high intensity and sustained in order to promote a significant collapse.

The link between rainfall and dome collapse therefore warrants further detailed study analogous to the work of Matthews et al. (2002) on Montserrat, along with modelling of the physical processes involved, in order to characterize the

conditions conducive to a rainfall-induced collapse and develop tools for monitoring and hazard mitigation. Systematic analysis of the rainfall intensities required to trigger pyroclastic flows, for example (as has been done for lahars at Pinatubo; Pierson et al., 1996), could contribute to hazard mitigation at dome-forming volcanoes in the tropics. At Merapi, a Doppler radar system has been used to measure the size and velocity of dome collapse pyroclastic flows and rockfalls from the active dome since October 2001, and the system also detects rainfall (Hort et al., 2002). Extended use of such an instrument could also illuminate the link between rainfall and lava dome instability.

One of the most remarkable aspects of the 20 March 2000 dome collapse was that it removed almost the entire lava dome that had been growing since November 1999. The post-collapse morphology of the dome region was thus similar to that observed prior to the beginning of phase 2 of dome growth, with a girdle of remnant dome material from 1995–1998 forming a semi-circular scar around the conduit region. Why the N99 dome was so efficiently removed by the collapse is not fully understood, but it may have been partly due to a mechanical contrast between the older 1995–1998 dome material and the 1999–2000 growth. The periphery of the N99 dome may have acted as a channel for rainwater, which infiltrated the dome and promoted failure along this bounding surface. The rain had little or no effect on the older 1995–1998 dome remnants since these were not noticeably altered by the 20 March 2000 activity; suggesting that the higher temperature of the N99 dome was an important factor in its response to the rainfall.

We also consider that the manner in which a dome grows must influence the style in which it collapses. Watts et al. (2002) have described the typical style of dome growth observed throughout the 1995–2003 SHV eruption, which involves the emplacement of individual lobes that grow in a particular orientation bounded by shear faults whilst shedding material from their headwall, before stagnating prior to a switch in extrusion direction. The switch in extrusion direction and subsequent propagation of a new upper conduit wall through the dome often prompted dome collapse in phase 1 of the eruption. These individual lobes or 'units' grow in sequence and therefore may also collapse in sequence, whilst varying styles and rates of dome growth may explain the variation in pyroclastic flow magnitudes during dome collapses at SHV, Merapi and Unzen. Furthermore, on the rare occasions that they have been observed, the interior of dome lobes have appeared highly fractured, which could promote penetration of water into the core of the dome and also helps to explain the rapid break-up of lobes as a collapse progresses (e.g. Sparks et al., 2000).

We have proposed that the highest-velocity pyroclastic flows generated in the latter stages of the 20 March 2000 collapse originated from the hot, gas-rich interiors of individual dome lobes as they were unroofed. These flows produced convective ash plumes or possibly small explosions that could be the origin of the ash pulses visible in satellite imagery prior to the emergence of the paroxysmal ash cloud (Fig. 6). Had the 20 March 2000 collapse not been channelled by the pre-existing 1995–1998 dome remnants and the TRV, these high velocity pyroclastic flows (and associated ash-cloud surges) could potentially have been directed down other flanks of the volcano, with serious hazard implications. At the time of writing (July 2003) the SHV dome has overtopped the 1995–1998 dome remnants in many locations, increasing the risk of pyroclastic flows in directions other than towards the east. Hence, for unconfined domes that exhibit similar growth patterns to those observed during the SHV eruption (Watts et al., 2002), continuous monitoring of extrusion directions is critical to the assessment of pyroclastic flow and surge hazards.

8. Summary

On 20 March 2000 the SHV lava dome that had been growing continuously since November 1999 was almost entirely removed by a series of pyroclastic flows that gradually increased in intensity over a ~4-h period, culminating in a short explosive phase. Peak discharge rates of pyroclastic flows at the climax of the collapse, estimated

from broadband seismic data, may have exceeded 20000 m^3 s^{-1}, and the flows were highly erosive. No significant geophysical precursors were recognized, but shortly before the first seismic signals associated with this dome collapse were received, intense rainfall developed over Montserrat, probably playing a role in the initiation and prolongation of the activity. Lahars also occurred on several flanks of the volcano during the collapse.

The link between rainfall and volcanic activity remains contentious and requires further study and observations, but the occurrence of three large dome collapses on Montserrat since 1998 (3 July 1998, 20 March 2000 and 29 July 2001) during periods of intense rain provides further compelling evidence for a link. Available rainfall data for the 20 March 2000 collapse are not sufficient to provide unequivocal evidence for a rainfall-induced event or to elucidate possible mechanisms, but it is becoming clear that during phase 2 of dome building on Montserrat there is an increased risk of dome collapses during periods of sustained, intense rainfall. This contrasts with phase 1 of dome growth, during which changes in pressurization and dome growth rate were the principal factors governing the incidence of dome collapse. Further studies at dome-forming volcanoes, using rain gauges with high temporal resolution (e.g. Matthews et al., 2002) or Doppler radar systems (e.g. Hort et al., 2002), could permit quantification of the rainfall rates necessary to initiate dome failure and thus contribute to hazard mitigation. Meteorological monitoring, to forecast impending tropical waves, hurricanes or storms, would be beneficial at active or recently active volcanoes in temperate or tropical regions.

Acknowledgements

We gratefully acknowledge all the MVO staff and visitors prior to and during March 2000 for observations and collection of the data presented in this paper. Adrian Matthews generously provided the rainfall data. Thorough reviews of the manuscript by Paul Cole and Arnold Brodscholl significantly improved the paper. The Government of Montserrat and the British Government (through the Department for International Development) supported the authors' work at the MVO. This paper is published by permission of the Director, British Geological Survey and the Director, MVO.

References

Abdurachman, E.K., Bourdier, J.-L., Voight, B., 2000. Nuées ardentes of 22 November 1994 at Merapi volcano, Java, Indonesia. J. Volcanol. Geotherm. Res. 100, 345–361.

Brodscholl, A., Kirbani, S.B., Voight, B., 2000. Sequential dome-collapse nuées ardentes analysed from broadband seismic data, Merapi Volcano, Indonesia. J. Volcanol. Geotherm. Res. 100, 363–369.

Calder, E.S., Cole, P.D., Dade, W.B., Druitt, T.H., Hoblitt, R.P., Huppert, H.E., Ritchie, L., Sparks, R.S.J., Young, S.R., 1999. Mobility of pyroclastic flows and surges at the Soufriere Hills Volcano, Montserrat. Geophys. Res. Lett. 26, 537–540.

Casadevall, T.J., 1994. The 1989–1990 eruption of Redoubt Volcano, Alaska – impacts on aircraft operations. In: Miller, T.P., Chouet, B.A. (Eds.), The 1989–1990 eruptions of Redoubt Volcano, Alaska. J. Volcanol. Geotherm. Res. 62, 301–316.

Christiansen, R.L., Peterson, D.W., 1981. Chronology of the 1980 eruptive activity. In: Lipman, P.W., Mullineaux, D.R. (Eds.), The 1980 Eruptions of Mount St. Helens, Washington. U.S. Geological Survey Professional Paper 1250, 844 pp.

Cole, P.D., Calder, E.S., Druitt, T.H., Hoblitt, R., Robertson, R., Sparks, R.S.J., Young, S.R., 1998. Pyroclastic flows generated by gravitational instability of the 1996–97 lava dome of Soufriere Hills Volcano, Montserrat. Geophys. Res. Lett. 25, 3425–3428.

Cole, P.D., Calder, E.S., Sparks, R.S.J., Clarke, A.B., Druitt, T.H., Young, S.R., Herd, R.A., Harford, C.L., Norton, G.E., 2002. Deposits from dome collapse and fountain collapse pyroclastic flows during 1996–99 at Soufriere Hills volcano, Montserrat. In: Druitt, T.H., Kokelaar, B.P. (Eds.), The Eruption of Soufrière Hills Volcano, Montserrat, from 1995 to 1999. Geological Society of London Memoir 21, pp. 231–262.

Denlinger, R.P., Hoblitt, R.P., 1999. Cyclic eruptive behaviour of silicic volcanoes. Geology 27, 459–462.

Druitt, T.H., Young, S.R., Baptie, B., Bonadonna, C., Calder, E.S., Clarke, A.B., Cole, P.D., Harford, C.L., Herd, R.A., Luckett, R., Ryan, G., Voight, B., 2002. Periodic vulcanian explosions and fountain collapse at the Soufrière Hills Volcano, Montserrat, 1997. In: Druitt, T.H., Kokelaar, B.P. (Eds.), The Eruption of Soufrière Hills Volcano, Montserrat, from 1995 to 1999. Geological Society of London Memoir 21, pp. 281–306.

Edmonds, M., Pyle, D., Oppenheimer, C., 2002. HCl emissions

at Soufrière Hills Volcano, Montserrat, West Indies, during a second phase of dome building: November 1999 to October 2000. Bull. Volcanol. 64, 21–30.
GVN, 1990. Santa María. Smithsonian Institution Global Volcanism Network Bull. 15 (11).
GVN, 1992a. Merapi. Smithsonian Institution Global Volcanism Network Bull. 17 (10).
GVN, 1992b. Merapi. Smithsonian Institution Global Volcanism Network Bull. 17 (11).
GVN, 1993a. Merapi. Smithsonian Institution Global Volcanism Network Bull. 18 (1).
GVN, 1993b. Guagua Pichincha. Smithsonian Institution Global Volcanism Network Bull. 18 (2).
GVN, 1994a. Merapi. Smithsonian Institution Global Volcanism Network Bull. 19 (1).
GVN, 1994b. Merapi. Smithsonian Institution Global Volcanism Network Bull. 19 (10).
GVN, 1997. Merapi. Smithsonian Institution Global Volcanism Network Bulletin, 22 (6).
Hammouya, G., Allard, P., Jean-Baptiste, P., Parello, F., Semet, M.P., Young, S.R., 1998. Pre- and syn-eruptive geochemistry of volcanic gases from Soufriere Hills of Montserrat, West Indies. Geophys. Res. Lett. 25, 3685–3688.
Harris, A.J.L., Flynn, L.P., Rothery, D.A., Oppenheimer, C., Sherman, S., 1999. Mass flux measurements at active lava lakes: Implications for magma recycling. J. Geophys. Res. 104, 7117–7136.
Hort, M., Seyfried, R., Ratdomopurbo, A., Sulistio, A., Brodscholl, A., Voege, M., Ruepke, L., 2002. Doppler radar observations at Merapi volcano, Indonesia: Insight into eruption mechanisms. EOS Trans. AGU 83 (47), Fall Meeting, Suppl., Abstract V22C-02.
Kays, W.M., Crawford, M.E., 1980. Convective Heat and Mass Transfer. McGraw-Hill, New York, 420 pp.
Kerle, N., van Wyk de Vries, B., 2001. The 1998 debris avalanche at Casita volcano, Nicaragua – investigation of structural deformation as the cause of slope instability using remote sensing. J. Volcanol. Geotherm. Res. 105, 49–63.
Mastin, L.G., 1993. Can rain cause volcanic eruptions? USGS Open-File Report 93–445 (http://vulcan.wr.usgs.gov/Projects/Mastin/Publications/OFR93-445/OFR93-445.html).
Mastin, L.G., 1994. Explosive tephra emissions at Mount St. Helens, 1989–1991 – the violent escape of magmatic gas following storms? Geol. Soc. Am. Bull. 106, 175–185.
Matthews, A.J., Barclay, J., Carn, S., Thompson, G., Alexander, J., Herd, R., Williams, C., 2002. Rainfall induced volcanic activity on Montserrat. Geophys. Res. Lett. 29 (13) (DOI: 10.1029/2002GL014863).
McKee, C.O., Wallace, D.A., Almond, R.A., Talai, B., 1981. Fatal hydro-eruption of Karkar volcano in 1979: Development of a maar-like crater. In: R.W. Johnson (Ed.), Cooke–Ravian Volume of Volcanological Papers. Geological Survey of Papua New Guinea Memoir 10, Libra Press, Hong Kong, pp. 63–84.
Miller, A.D., Stewart, R.C., White, R.A., Luckett, R., Baptie, B.J., Aspinall, W.P., Latchman, J.L., Lynch, L.L., Voight, B., 1998. Seismicity associated with dome growth and collapse at the Soufriere Hills Volcano, Montserrat. Geophys. Res. Lett. 25, 3401–3404.
Miller, T.P., Chouet, B., 1994. The 1989–1990 eruptions of Redoubt Volcano: An introduction. J. Volcanol. Geotherm. Res. 62, 1–10.
Nakada, S., 2000. Hazards from pyroclastic flows and surges. In: Sigurdsson, H., Houghton, B.F., McNutt, S.R., Rymer, H., Stix, J. (Eds.), Encyclopedia of Volcanoes. Academic Press, San Diego, CA, pp. 945–955.
Neuberg, J., 2000. External modulation of volcanic activity. Geophys. J. Int. 142, 232–240.
Newhall, C.G., Melson, W.G., 1983. Explosive activity associated with the growth of volcanic domes. J. Volcanol. Geotherm. Res. 17, 111–131.
Norris, R.D., 1994. Seismicity of rockfalls and avalanches at three Cascade Range volcanoes: Implications for seismic detection of hazardous mass movements. Bull. Seismol. Soc. Am. 84, 1925–1939.
Norton, G.E., Watts, R.B., Voight, B., Mattioli, G.S., Herd, R.A., Young, S.R., Devine, J.D., Aspinall, W.P., Bonadonna, C., Baptie, B.J., Edmonds, M., Harford, C.L., Jolly, A.D., Loughlin, S.C., Luckett, R., Sparks, R.S.J., 2002. Pyroclastic flow and explosive activity at Soufrière Hills Volcano, Montserrat, during a period of virtually no magma extrusion (March 1998 to November 1999). In: Druitt, T.H., Kokelaar, B.P. (Eds.), The Eruption of Soufrière Hills Volcano, Montserrat, from 1995 to 1999. Geological Society of London Memoir 21, pp. 467–482.
Oppenheimer, C., 1991. Lava flow cooling estimated from Landsat Thematic Mapper infrared data: The Lonquimay eruption (Chile, 1989). J. Geophys. Res. 96, 21865–21878.
Perret, F.A., 1937. The eruption of Mt. Pelée 1929–32. Carnegie Institution of Washington, Washington, DC.
Pierson, T.C., Daag, A.S., Delos Reyes, P.J., Regalado, M.T.M., Solidum, R.U., Tubianosa, B.S., 1996. Flow and deposition of posteruption hot lahars on the east side of Mount Pinatubo, July–October 1991. In: Newhall, C.G., Punongbayan, R.S. (Eds.), Fire and Mud: Eruptions and Lahars of Mount Pinatubo, Philippines. University of Washington Press, Seattle, pp. 921–950.
Ratdomopurbo, A., Poupinet, G., 2000. An overview of the seismicity of Merapi volcano (Java, Indonesia), 1983–1994. J. Volcanol. Geotherm. Res. 100, 193–214.
Robertson, R., Cole, P., Sparks, R.S.J., Harford, C., Lejeune, A.M., McGuire, W.J., Miller, A.D., Murphy, M.D., Norton, G., Stevens, N.F., Young, S.R., 1998. The explosive eruption of Soufriere Hills Volcano, Montserrat, West Indies, 17 September, 1996. Geophys. Res. Lett. 25, 3429–3432.
Rose, W.I., Mayberry, G.C., 2000. Use of GOES thermal infrared imagery for eruption scale measurements, Soufriere Hills, Montserrat. Geophys. Res. Lett. 27, 3097–3100.
Sato, H., Fujii, T., Nakada, S., 1992. Crumbling of dacite dome lava and generation of pyroclastic flows at Unzen volcano. Nature 360, 664–666.
SEAN, 1984. Merapi. Smithsonian Institution Scientific Event Alert Network 9 (6).

Sparks, R.S.J., 1997. Causes and consequences of pressurization in lava dome eruptions. Earth Planet. Sci. Lett. 150, 177–189.

Sparks, R.S.J., Murphy, M., Lejeune, A.-M., Watts, R.B., Barclay, J., Young, S.R., 2000. Control on the emplacement of the andesite lava dome of the Soufriere Hills volcano, Montserrat by degassing-induced crystallization. Terra Nova 12, 14–20.

Voight, B., Elsworth, D., 2000. Instability and collapse of hazardous gas-pressurized lava domes. Geophys. Res. Lett. 27, 1–4.

Voight, B., Hoblitt, R.P., Clarke, A.B., Lockhart, A.B., Miller, A.D., Lynch, L., McMahon, J., 1998. Remarkable cyclic ground deformation monitored in real-time on Montserrat, and its use in eruption forecasting. Geophys. Res. Lett. 25, 3405–3408.

Voight, B., Sparks, R.S.J., Miller, A.D., Stewart, R.C., Hoblitt, R.P., Clarke, A., Ewart, J., Aspinall, W.P., Baptie, B., Calder, E.S., Cole, P., Druitt, T.H., Harford, C., Herd, R.A., Jackson, P., Lejeune, A.M., Lockhart, A.D., Loughlin, S.C., Luckett, R., Lynch, L., Norton, G.E., Robertson, R., Watson, I.M., Watts, R., Young, S.R., 1999. Magma flow instability and cyclic activity at Soufrière Hills Volcano, Montserrat, British West Indies. Science 283, 1138–1142.

Voight, B., Constantine, E.K., Siswowidjoyo, S., Torley, R., 2000a. Historical eruptions of Merapi Volcano, Central Java, Indonesia, 1768–1998. J. Volcanol. Geotherm. Res. 100, 69–138.

Voight, B., Young, K.D., Hidayat, D., Subandrio Purbawinata, M.A., Ratdomopurbo, A., Suharna Panut Sayudi, D.S., LaHusen, R., Marso, J., Murray, T.L., Dejean, M., Iguchi, M., Ishihara, K., 2000b. Deformation and seismic precursors to dome-collapse and fountain-collapse nuées ardentes at Merapi Volcano, Java, Indonesia, 1994–1998. J. Volcanol. Geotherm. Res. 100, 261–287.

Watts, R.B., Herd, R.A., Sparks, R.S.J., Young, S.R., 2002. Growth patterns and emplacement of the andesitic lava dome at Soufrière Hills volcano, Montserrat. In: Druitt, T.H., Kokelaar, B.P. (Eds.), The Eruption of Soufrière Hills Volcano, Montserrat, from 1995 to 1999. Geological Society of London Memoir 21, pp. 115–142.

Woods, A.W., Sparks, R.S.J., Ritchie, L.I., Batey, J., Gladstone, C., Bursik, M.I., 2002. The explosive decompression of a pressurised volcanic dome: The 26 December 1997 collapse and explosion of Soufriere Hills Volcano, Montserrat. In: Druitt, T.H., Kokelaar, B.P. (Eds.), The Eruption of Soufrière Hills Volcano, Montserrat, from 1995 to 1999. Geological Society of London Memoir 21, pp. 457–466.

Yamamoto, T., Takarada, S., Suto, S., 1993. Pyroclastic flows from the 1991 eruption of Unzen volcano, Japan. Bull. Volcanol. 55, 166–175.

Yamasato, H., Kitagawa, S., Komiya, M., 1997. Effect of rainfall on dacitic lava dome collapse at Unzen volcano, Japan. Papers Meteorol. Geophys. 48.

Young, S.R., Sparks, R.S.J., Aspinall, W.P., Lynch, L.L., Miller, A.D., Robertson, R.E.A., Shepherd, J.B., 1998. Overview of the eruption of Soufriere Hills volcano, Montserrat, 18 July 1995 to December 1997. Geophys. Res. Lett. 25, 3389–3392.